Mesenteric Fat Lipolysis Mediates Obesity-associated Hepatic Steatosis and Insulin Resistance

Wueest, Stephan ; Item, Flurin ; Lucchini, Fabrizio C ; Challa, Tenagne D ; Müller, Werner ; Blüher, Matthias ; Konrad, Daniel

Abstract: Hepatic steatosis and insulin resistance are among the most prevalent metabolic disorders and tightly associated with obesity and type 2 diabetes. However, underlying mechanism linking obesity to hepatic lipid accumulation and insulin resistance are incompletely understood. Glycoprotein 130 (gp130) is the common signal transducer of all interleukin 6 (IL-6) cytokines. Herein, we provide evidence that gp130-mediated adipose tissue lipolysis promotes hepatic steatosis and insulin resistance. In obese mice, adipocyte-specific gp130 deletion reduced basal lipolysis and enhanced insulin's ability to suppress lipolysis from mesenteric but not epididymal adipocytes. Consistently, free fatty acid levels were reduced in portal but not in systemic circulation of obese knockout mice. Importantly, adipocyte-specific gp130 knockout mice were protected from high fat diet (HFD)-induced hepatic steatosis as well as insulin resistance. In humans, omental but not subcutaneous IL-6 mRNA expression correlated positively with liver lipid accumulation ($r=0.31$; $p<0.05$) and negatively with euglycemic clamp glucose infusion rate ($r=-0.28$; $p<0.05$). Our results demonstrate that IL-6 cytokine-induced lipolysis may be restricted to mesenteric WAT and that it contributes to hepatic insulin resistance and steatosis. Therefore, blocking IL-6 cytokine signaling in (mesenteric) adipocytes may be a novel approach to blunt detrimental fat-liver crosstalk in obesity.

DOI: https://doi.org/10.2337/db15-0941

Mesenteric Fat Lipolysis Mediates Obesity-associated Hepatic Steatosis and Insulin Resistance

Stephan Wueest[1,2], Flurin Item[1,2], Fabrizio C. Lucchini[1,2,3], Tenagne D. Challa[1,2], Werner Müller[4], Matthias Blüher[5] and Daniel Konrad[1,2,3]

[1]Division of Pediatric Endocrinology and Diabetology and [2]Children Research's Centre, University Children's Hospital, Zurich, Switzerland

[3]Zurich Center for Integrative Human Physiology, University of Zurich, Zurich, Switzerland

[4]Faculty of Life Sciences, University of Manchester, Manchester, U.K.

[5]University of Leipzig, Department of Medicine, Leipzig, Germany

All correspondence and requests for reprint to:

Daniel Konrad, MD PhD

University Children's Hospital

Department of Endocrinology and Diabetology

Steinwiesstrasse 75

CH-8032 Zurich

Tel: ++41-44-266 7966; Fax: ++41-44-266 7983

Email: daniel.konrad@kispi.uzh.ch

or:

Stephan Wueest, PhD

Email: stephan.wueest@usz.ch

Diabetes Publish Ahead of Print, published online September 17, 2015

Abstract

Hepatic steatosis and insulin resistance are among the most prevalent metabolic disorders and tightly associated with obesity and type 2 diabetes. However, underlying mechanism linking obesity to hepatic lipid accumulation and insulin resistance are incompletely understood. Glycoprotein 130 (gp130) is the common signal transducer of all interleukin 6 (IL-6) cytokines. Herein, we provide evidence that gp130-mediated adipose tissue lipolysis promotes hepatic steatosis and insulin resistance. In obese mice, adipocyte-specific gp130 deletion reduced basal lipolysis and enhanced insulin's ability to suppress lipolysis from mesenteric but not epididymal adipocytes. Consistently, free fatty acid levels were reduced in portal but not in systemic circulation of obese knockout mice. Importantly, adipocyte-specific gp130 knockout mice were protected from high fat diet (HFD)-induced hepatic steatosis as well as insulin resistance. In humans, omental but not subcutaneous *IL-6* mRNA expression correlated positively with liver lipid accumulation ($r=0.31$; $p<0.05$) and negatively with euglycemic clamp glucose infusion rate ($r=-0.28$; $p<0.05$). Our results demonstrate that IL-6 cytokine-induced lipolysis may be restricted to mesenteric WAT and that it contributes to hepatic insulin resistance and steatosis. Therefore, blocking IL-6 cytokine signaling in (mesenteric) adipocytes may be a novel approach to blunt detrimental fat-liver crosstalk in obesity.

Introduction

The prevalence of obesity and associated diseases such as insulin resistance and hepatic steatosis are increasing to epidemic proportions (1). Yet, underlying pathological mechanisms are not fully understood. Although there is evidence that interleukin-6 (IL-6) may contribute to the development of fatty liver disease and hepatic insulin resistance, its exact role in the pathogenesis of these disorders is the subject of intense debate (2-5). IL-6 is secreted by different cells and tissues such as adipocytes, immune cells and skeletal muscle thereby modulating metabolism under both physiological and pathophysiological conditions (2; 6). To activate its intracellular signaling pathways, IL-6 either binds to its membrane-bound receptor (mIL-6R; classic signaling) or to its soluble receptor (sIL-6; trans-signaling pathway). Of note, mIL-6R is expressed in the liver and immune cells while it is absent in adipocytes (7). In turn, this ligand/receptor complex associates with a homodimer of glycoprotein 130 (gp130), which is a common signal transducer protein of all IL-6 cytokines (8; 9). Subsequently, the JAK/STAT and the ERK1/2 pathway are activated (9; 10).

In the liver, chronically elevated circulating IL-6 levels were proposed to induce insulin resistance and inflammation in mice (11; 12). In contrast, a recent study proposed the opposite since it found IL-6 to reduce inflammation and to improve insulin sensitivity in the liver (13). Therefore, the hepatic derangements associated with elevated IL-6 levels as observed in the former studies (11; 12) may be mediated via an indirect effect of IL-6, for example through induction of adipose tissue lipolysis. Indeed, IL-6 was shown to induce lipolysis *in vivo* and *in vitro* (14; 15) and a recent publication suggested that IL-6 promotes hepatic insulin resistance indirectly through increased free fatty acid (FFA) release from adipose tissue in rodents (16). Of note, obesity-induced IL-

6 increase was higher in mesenteric fat compared to other adipose depots (17; 18) suggesting that IL-6-induced adipose tissue lipolysis may play a distinct role in visceral fat.

In the present study, we sought to determine whether (i) mesenteric adipose tissue is more sensitive to IL-6 -induced lipolysis than epididymidal fat and whether (ii) IL-6-induced FFA-release from (mesenteric) fat contributes to obesity-associated hepatic steatosis and insulin resistance making use of adipocyte-specific gp130 depleted mice.

Research Design and Methods

Determination of total liver fat and adipose tissue IL-6 mRNA expression in humans

IL-6 mRNA expression was measured in abdominal omental and subcutaneous adipose tissue (AT) samples obtained in parallel from 63 men (n = 34) and women (n = 29) who underwent open abdominal surgery for Roux-en-Y bypass, sleeve gastrectomy, explorative laparotomy or elective cholecystectomy. Liver and AT biopsies was taken during surgery, immediately snap-frozen in liquid nitrogen, and stored at −80°C until further preparations. Measurement of total body and liver fat, tissue sample handling and analysis of blood samples including measurement of serum adiponectin and leptin concentrations has been performed as described previously (19; 20). IL-6 plasma concentrations were measured by a high-sensitivity ELISA kit (Quantikine IL-6, R&D Systems, Oxford, UK). Insulin sensitivity was assessed with the euglycemic-hyperinsulinemic clamp method using a previously described protocol (21). Glucose infusion rate (GIR) was calculated from the last 45 min of the clamp, during which

glucose infusion rate could be kept constant in order to achieve the target plasma glucose concentration of 5.5 (± 5%) mmol/L. Therefore, the duration of the clamp varied between individuals (range 120-200min). GIR was normalized to lean body mass. In premenopausal women, clamp studies were performed during the luteal phase of the menstrual cycle. All participants gave their written informed consent before taking part in the study. All investigations have been approved by the ethics committee of the University of Leipzig (363-10-13122010 and 017-12-230112) and were carried out in accordance with the Declaration of Helsinki.

Human *IL-6* mRNA expression was measured by qRT-PCR using Assay-on-Demand gene expression kit (Hs00985639_m1; Applied Biosystems, Darmstadt, Germany), and fluorescence was detected on an ABI PRISM 7000 Sequence Detector (Applied Biosystems). *IL-6* mRNA expression was calculated relative to the mRNA expression of *HPRT1* mRNA (Hs01003267_m1; Applied Biosystems).

Animals

Adipocyte-specific gp130 knockout mice ($gp130^{\Delta adipo}$) on a C57BL/6J background were generated by crossing gp130 floxed ($gp130^{F/F}$) mice (22) to animals expressing the Cre recombinase controlled by the Adipoq promoter (AdipoqCre mice; purchased from The Jackson Laboratory).

Six weeks-old male mice were fed *ad libitum* with standard rodent diet (chow) or high fat diet (HFD; D12331, Research Diets, New Brunswick, USA) for 12 weeks. HFD consisted of 58% of calories derived from fat, 28% from carbohydrate and 16% from protein. All protocols conformed to the Swiss animal protection laws and were approved by the Cantonal Veterinary Office in Zurich, Switzerland.

Glucose clamp studies

Glucose clamp studies were performed as described (23). Clamps were performed in freely moving mice. Glucose infusion rate was calculated once glucose infusion reached a more or less constant rate with blood glucose levels at 5 mmol/l (80–90 min after the start of insulin infusion). Thereafter, blood glucose was kept constant at 5 mmol/l for 15-20 min and glucose infusion rate was calculated. The glucose disposal rate was calculated by dividing the rate of [3-^{3}H]glucose infusion by the plasma [3-^{3}H]glucose specific activity (24; 25). Endogenous glucose production during the clamp was calculated by subtracting the glucose infusion rate from the glucose disposal rate (24; 25). In order to assess tissue specific glucose uptake, a bolus (10 µCi) of 2-[1-^{14}C]deoxyglucose was administered via catheter at the end of the steady state period. Blood was sampled 2, 15, 25 and 35 min after bolus delivery. Area under the curve of disappearing plasma 2-[1-^{14}C]deoxyglucose was used together with tissue-concentration of phosphorylated 2-[1-^{14}C]deoxyglucose to calculate glucose uptake.

Lipolysis assays

Adipocytes were isolated and lipolysis was assessed as described (26). Isolated adipocytes were incubated in the absence or presence of 100 nM insulin, 100 ng/ml recombinant murine IL-6 (R&D Systems, Oxford, UK) or 1 µM isoproterenol (Sigma, Buchs, Switzerland) for one hour. FFA levels were measured using the ACS-ACOD-MEHA method from Wako Chemicals GmbH (Neuss, Germany).

Cell size determination

Cell size of isolated adipocytes was analyzed by a Multisizer™ 3 Coulter Counter® as previously described (27).

Blood sampling

Immediately after euthanasia abdominal cavity was opened and the portal vein exposed. It was punctured by a syringe (0.30mm (30G) x 8mm; BD, New Jersey, USA) and the blood was collected. Systemic blood was sampled after cardiac puncture using similar syringes. Blood was added to an Eppendorf tube with a final concentration of 5 mM EDTA. After centrifugation, plasma was stored at -80°C upon further processing.

Determination of plasma insulin, triglyceride and free fatty acids

Plasma triglyceride (TG) and free fatty acid (FFA) levels were determined as described elsewhere (28). Plasma insulin levels were measured using an ELISA kit as described previously (29).

Western blotting

Liver or adipose tissue samples were homogenized and Western blotting was performed as described previously (30). The following primary antibodies were used: anti-gp130, anti-SOCS3 (Santa Cruz Biotechnology, Dallas, TX, USA), anti-phospho p38, anti-phospho ERK, anti-ERK (Cell Signaling, Danvers, MA, USA) and anti-actin (Millipore, Billerica, MA, USA). Membranes were exposed in an Image Reader and analyzed with Image Analyzer (FujiFilm, Dielsdorf, Switzerland).

RNA extraction and quantitative reverse transcription-PCR (RT-PCR)

Total RNA was extracted using RNeasy Lipid Tissue Mini Kit (Qiagen, Basel, Switzerland) and concentration was determined spectrophotometrically (Nanodrop 1000; Nanodrop Technologies, Boston, MA). 1 µg of RNA were reverse transcribed with Superscript III Reverse Transcriptase (Invitrogen, Basel, Switzerland) using random hexamer primer (Invitrogen). Taqman (Applied Biosystems, Rotkreuz, Switzerland) was used for real-time PCR amplification. The following PCR primers (Applied Biosystems) were used: TNF-α Mm00443258_m1, IL-6 Mm00446190_m1, F4/80 Mm00802529_m1, CD11b Mm00434455_m1, FAS Mm00662319_m1, PPARα Mm00627559_m1, SREBP1 Mm00550338_m1, SCD-1 Mm01197142_m1, CPT-1 Mm00550438_m1, AOX Mm00443579_m1. Relative gene expression was obtained after normalization to 18sRNA (Applied Biosystems), using the formula $2^{-\Delta\Delta cp}$ (31).

Liver triglyceride and total lipid determination

Liver tissue (20-30mg) was homogenized in PBS and lipids were extracted in a chloroform-methanol (2:1) mixture. Total liver lipids were determined by a sulfophosphovanillin reaction as previously described (32). Liver triglyceride levels were determined in 50 mg of liver tissue according to the method of Bligh and Dyer (33) and quantified with an enzymatic assay (Roche Diagnostics, Rotkreuz, Switzerland).

Histology

Liver tissues were fixed in 4% buffered formalin and embedded in paraffin. Sections were cut and stained with hematoxylin and eosin.

Data analysis

Statistical analyses were performed using Student's *t* test or ANOVA with Newman-Keuls post-hoc test. In human studies, linear relationships were assessed by Spearman Rank correlation analyses. p-Values < 0.05 were considered significant.

Results

Similar weight gain and adipogenesis in adipocyte-specific gp130 knockout mice and control littermates

To investigate the role of IL-6-induced lipolysis in metabolic derangements *in vivo*, we generated adipocyte-specific gp130 knockout mice ($gp130^{\Delta adipo}$) using the cre-lox system. As controls, littermate mice with floxed gp130 but absent Cre-recombinase expression were used ($gp130^{F/F}$). While we are aware of the fact that knockout of gp130 in adipocytes affects the signaling pathway of all members of the IL-6 cytokines, it still seems to be an adequate mouse model to investigate our hypothesis as the mIL-6R is not expressed in adipocytes (7), precluding cell-specific depletion of IL-6 signaling in adipocytes similar to liver-specific IL-6R knockout mice (13). As expected, gp130 protein levels were highly reduced in isolated adipocytes of $gp130^{\Delta adipo}$ mice, decreased in white adipose tissue (WAT), which also contains non-adipocyte cell types, but unchanged in skeletal muscle and liver compared to control mice (Figure 1A). To induce obesity, 6 weeks old mice were either fed a control chow or a HFD for 12 weeks. As expected, HFD feeding increased body and fat pad weights, whereas lack of IL-6 cytokine signaling in adipocytes did not affect body weight or adipogenesis as assessed by fat

pad weights and adipocyte size (Figures 1B to 1F). Likewise, protein levels of PPARγ in epididymal and mesenteric WAT were similar in both genotypes (data not shown). Thus, adipocyte-specific gp130 deficiency did neither affect HFD-induced increase in body and fat pad weight nor adipogenesis.

Reduced basal lipolysis and portal FFA levels in obese gp130$^{\Delta adipo}$ mice

In order to assess the impact of IL-6 cytokine signaling on lipolytic activity, FFA release was analyzed in adipocytes isolated from gp130 knockout and control littermates. Compared to chow-fed mice, basal lipolysis was significantly increased in epididymal and mesenteric adipocytes of obese control mice (Figures 2A and 2B). Importantly, basal FFA release was blunted in mesenteric but not epididymal adipocytes isolated from obese gp130$^{\Delta adipo}$ mice (Figures 2A and 2B), suggesting that IL-6 cytokine signaling contributes to enhanced FFA release from mesenteric adipocytes during obesity. Functionality of isolated adipocytes was confirmed by increased lipolysis after stimulation with the beta-adrenergic receptor agonist isoproterenol in all depots examined (Supplemental Figures 1A and 1B). Of note, phosphorylation of ERK was significantly reduced in mesenteric but not epididymal WAT of obese knockout mice, supporting the notion that IL-6 cytokine-induced lipolysis *in vivo* is mediated by ERK (Figure 2C and 2D) confirming previous findings in adipocytes *in vitro* (15). *Ex vivo* findings of reduced lipolysis in portally-drained mesenteric adipocytes were confirmed *in vivo*, as the obesity-induced increase in circulating FFA levels was blunted in portal but not systemic circulation of knockout mice (Figures 2E and 2F). Importantly and in contrast to lipolysis, gp130 depletion did not affect IL-6 mRNA expression in mesenteric WAT (Figure 2G), suggesting similar portal delivery of IL-6 to the liver in both genotypes.

In addition, there was no major change in transcript levels of the macrophage markers CD11b and F4/80 (34) (Fig. 2H), suggesting similar macrophage content between both genotypes. Taken together, IL-6 cytokine signaling stimulates lipolysis of portally drained mesenteric but not of systemically drained epididymal fat.

Reduced hepatic steatosis in HFD-fed gp130$^{\Delta adipo}$ mice

Mesenteric (and omental) adipose tissue is mainly drained via the portal vein to the liver (35), where FFAs were previously reported to activate the stress kinase p38 mitogen-activated protein kinase (MAPK) (36; 37). Supporting such notion, phosphorylation of the p38 MAPK was reduced in livers of obese gp130$^{\Delta adipo}$ mice (Figure 3A). In contrast, mRNA expression of suppressor of cytokine signaling 3 (SOCS3), which can be induced in the liver by IL-6 thereby promoting hepatic insulin resistance (38), was similar in HFD-fed gp130$^{\Delta adipo}$ and control littermates (1.0±0.3 in gp130$^{F/F}$ mice vs. 1.2±0.2 in gp130$^{\Delta adipo}$ mice, p=0.7). In addition, SOCS3 protein levels were not different between both groups (Figure 3B). Such finding supports the notion of similar portal delivery of IL-6 to the liver in both gp130$^{\Delta adipo}$ and control mice. Importantly, WAT lipolysis is thought to be an important source of FFA leading to hepatic steatosis (39). Accordingly, it was suggested that in humans up to 59% of FFA bound in liver triglycerides (TG) may arise from plasma FFA (40). In line, the observed reduction of mesenteric WAT lipolysis in obese gp130$^{\Delta adipo}$ mice was associated with a significant decrease in hepatic steatosis as determined by total liver lipid and TG content (Figures 3C and 3D) as well as by histological examination (Figure 3E). Importantly and as expected, HFD feeding significantly increased hepatic lipid accumulation (Figures 3C and 3D). Of note, circulating TG content was similar between the genotypes (80.5±3.7

mg/dl in HFD-fed gp130$^{F/F}$ mice vs. 84.1±3.8 mg/dl in HFD-fed gp130$^{\Delta adipo}$ mice, p=0.5). Besides FFA uptake, hepatic lipid content is influenced by *de novo* lipogenesis and beta-oxidation (39-41). Therefore, hepatic mRNA expression of enzymes involved in lipogenesis and beta-oxidation were determined in HFD-fed mice, which was similar between both genotypes (Figure 3F). Such data further support the assumption that the reduced FFA flux is probably responsible for the observed decrease in hepatic lipid accumulation of knockout mice. Of note, there was no difference in hepatic mRNA levels of IL-6, TNFα and F4/80 suggesting a similar degree of hepatic inflammation in knockout and control mice (Figure 3B).

Improved hepatic insulin sensitivity in HFD-fed gp130$^{\Delta adipo}$ mice

Steatosis is closely associated with liver insulin resistance that may be also affected by WAT lipolysis (39). In this regard, increased portal delivery of FFA may induce liver insulin resistance via the accumulation of lipid metabolites and/or hepatic acetyl CoA or directly via activation of p38 MAPK (16; 36; 37; 42). Indeed and as mentioned above, phosphorylation of p38 MAPK was decreased in livers of obese gp130$^{\Delta adipo}$ (Figure 3A). To assess hepatic insulin sensitivity, hyperinsulinemic-euglycemic clamp studies were performed. HFD-fed gp130$^{\Delta adipo}$ mice revealed significantly improved insulin sensitivity as determined by higher glucose infusion rate (GIR) during hyperinsulinemic-euglycemic clamp studies (Figure 4A and Supplemental Figures 2A to 2C). Insulin-induced suppression of endogenous glucose production (mainly reflecting hepatic glucose production) was significantly higher in HFD-fed gp130$^{\Delta adipo}$ compared to gp130$^{F/F}$ mice (Figure 4B) indicating improved hepatic insulin sensitivity in knockout mice. In contrast, glucose uptake capacity into skeletal muscle

was not affected (Figure 4C). In addition, gp130 depletion had no impact on insulin's ability to suppress FFA release from isolated epididymal adipocytes (Figure 4D). In contrast and in support of depot-specific differences in adipocyte metabolism with regard to IL-6 cytokine action, insulin's ability to blunt lipolysis was significantly improved in mesenteric adipocytes isolated from obese knockout compared to control mice (Figure 4E).

Positive correlation of omental IL-6 expression with hepatic steatosis and insulin resistance in humans

Similar to observations in rodents, IL-6 expression was elevated in visceral/omental compared to subcutaneous fat depots in obese humans (43). Moreover, increased omental but not subcutaneous lipolysis was linked to obesity-induced fatty liver disease in morbidly obese humans (44). To unravel whether IL-6-induced omental fat lipolysis may contribute to obesity-associated hepatic steatosis and insulin resistance, *IL-6* mRNA expression was analyzed in adipose tissue of lean (n= 12, BMI 24.5±0.2 kg/m²) and overweight or obese (n=51, BMI 34.4±0.8 kg/m²) individuals and correlated to liver fat content. Basic clinical characteristics of these subjects are provided in Table 1. Supporting previous findings (43), *IL-6* mRNA was increased in omental, but not subcutanous adipose tissue of obese when compared to lean individuals (Figure 5A). Intriguingly, we found a significant positive correlation between omental ($r=0.31$; $p<0.05$) but not subcutaneous ($r=0.09$; $p=0.49$) *IL-6* expression and hepatic steatosis (Figure 5B and Supplemental Figure 3A). In addition, glucose infusion rate (GIR) during hyperinsulinemic-euglycemic clamp studies revealed significant negative correlation to omental but not subcutaneous *IL-6* mRNA expression (Figure 5C

and Supplemental Figure 3B). Of note, there was a significant correlation between liver fat content and clamp GIR ($r=-0.53$, $p<0.001$). These data support a role for omental IL-6 in the development of obesity-associated hepatic steatosis as well as insulin resistance in humans.

Discussion

The present study suggests that IL-6 signaling-mediated lipolysis may be restricted to omental/mesenteric adipose tissue and that it contributes to hepatic insulin resistance and steatosis. Such notion is based on the following findings: **i.** lipolysis from mesenteric but not epididymidal adipose tissue is reduced in HFD-fed gp130$^{\Delta adipo}$ mice compared to control littermates; **ii.** gp130 depletion specifically in adipocytes reduced both HFD-induced hepatic insulin resistance and steatosis.

IL-6 plays complex roles in inflammation and metabolism having both beneficial and adverse properties. In support of detrimental effects of IL-6, it was very recently shown that IL-6 induces FFA release in obesity, thereby contributing to increased hepatic glucose production and, hence, hepatic insulin resistance (16). Our findings presented herein would suggest that the IL-6 signaling-mediated increase in lipolysis is restricted to the portally drained mesenteric adipose tissue depot since depletion of gp130, the common signal transducer of IL-6, reduced FFA release only from isolated mesenteric but not epididymal adipocytes. As IL-6 is the gp130 cytokine with the best-known lipolytic function (9), such finding may be explained by an increased sensitivity of mesenteric adipocytes to IL-6-mediated lipolysis. However, IL-6-induced FFA release was only slightly elevated in mesenteric compared to epididymal adipocytes isolated

from wild-type mice (1.25±0.14 fold in mesenteric *vs.* 1.12±0.02 fold in epididymal, p=0.4). Alternatively, a selective obesity-induced increase in IL-6 content of mesenteric WAT may be responsible for the observed difference (17; 18). The later may be the result of unique endogenous properties of mesenteric WAT and/or depend on the close proximity to the gut leading to more pronounced inflammation in mesenteric/omental compared to other fat depots (35). Along this line, the staphylococcal enterotoxin A (SEA) was reported to bind to gp130 in adipocytes thereby interfering with insulin sensitivity and lipolysis (45). Interestingly, *Staphylococcal spp*. is detectable in gut microbiota and translocation of intestinal bacteria to mesenteric WAT was observed upon high fat feeding in mice (46; 47). Clearly, further studies are needed to unravel a potential involvement of SEA in obesity-induced adipose tissue lipolysis.

Besides IL-6, other cytokines signaling via gp130 may have contributed to the observed phenotype. Of note, several IL-6 cytokines were shown to individually affect differentiation and adipogenesis rendering gp130 a potential therapeutic target to combat obesity and its associated diseases (9). Accordingly, it was recently shown that blocking IL-6 trans-signaling using a soluble gp130Fc protein reduces obesity-induced infiltration of macrophages into adipose tissue (48). We found herein that lack of IL-6 cytokine signaling in adipocytes had no impact on fat mass and adipocyte size. Such observation may suggest that IL-6 cytokine signaling does not affect adipogenesis. However, Cre expression in our mouse model was under the control of the adiponectin promoter and, hence, only induced during late stages of adipocyte differentiation since it is located downstream of C/EBP (49). Thus, potential effects of individual IL-6 cytokines on early adipocyte differentiation (9) may not be reflected in $gp130^{\Delta adipo}$ mice.

Chronically elevated circulating IL-6 levels were proposed to contribute to obesity-associated hepatic inflammation and insulin resistance in mice (11; 12). In contrast, IL-6 was recently reported to reduce inflammation and to improve insulin sensitivity in liver (13). Our findings may propose an indirect negative impact of IL-6 on hepatic insulin resistance and steatosis through induction of adipose tissue lipolysis mainly in mesenteric/omental fat depots. Accordingly, depletion of IL-6 cytokine signaling in adipocytes reduced portal FFA concentration and improved hepatic lipid accumulation as well as insulin resistance in mice. Moreover, omental (but not subcutaneous) IL-6 expression correlated with hepatic steatosis and insulin resistance in humans. Since it was recently shown that increased omental (but not subcutaneous) lipolysis was linked to obesity-induced fatty liver disease in morbidly obese humans (44) and that visceral lipolysis may contribute significantly to the portal delivery of FFA to the liver (50) our proposed mechanism may be conserved between species. Besides reduced lipolysis, lower intestinal absorption of FFA (35) or increased fatty acid uptake by adipocytes may have contributed to decreased portal FFA levels in HFD-fed gp130$^{\Delta adipo}$ mice. While our data suggest that increased mesenteric FFA release into the portal vein impairs liver metabolism, such direct link may be questioned (51). Clearly, changed release of other non-FFA factors into portal and/or systemic circulation may have also contributed to the observed hepatic phenotype in obese gp130$^{\Delta adipo}$ mice.

In conclusion, the obesity-associated rise in mesenteric/omental adipose tissue IL-6 cytokine signaling promotes FFA release into the portal circulation inducing hepatic steatosis and/or insulin resistance. Hence, blocking IL-6 cytokine signaling in adipocytes may be a novel approach to blunt detrimental fat-liver crosstalk in obesity. To this end,

the development of cell-specific adeno-associated virus (AAV) vectors may be a promising tool in the future (52; 53).

Acknowledgements

This work was supported by research grants from the Swiss National Science Foundation (# 310030_160129) (to DK), the Olga Mayenfisch Stiftung, Zurich (to SW), and a grant from Deutsche Forschungsgemeinschaft the SFB 1052/1: “Obesity mechanisms” (to MB). We would like to thank Proff. Eugen Schoenle and Giatgen Spinas for continuous support and Ms. Alexandra Grob for help regarding mouse breeding and genotyping.

Author Contributions

SW and DK conceived the study and wrote the paper. SW, FI, FCL, TDC and MB performed the experimental work. WM provided gp130$^{\Delta adipo}$ mice and gave conceptual advice. All authors contributed to discussion and reviewed/edited manuscript.

Conflict of interests’ statement

All authors state no conflict of interest.

References

1. Lazo M, Hernaez R, Eberhardt MS, Bonekamp S, Kamel I, Guallar E, Koteish A, Brancati FL, Clark JM: Prevalence of nonalcoholic fatty liver disease in the United States: the Third National Health and Nutrition Examination Survey, 1988-1994. *Am J Epidemiol* 178:38-45, 2013
2. Carey AL, Febbraio MA: Interleukin-6 and insulin sensitivity: friend or foe? *Diabetologia* 47:1135-1142, 2004
3. Carter-Kent C, Zein NN, Feldstein AE: Cytokines in the pathogenesis of fatty liver and disease progression to steatohepatitis: implications for treatment. *Am J Gastroenterol* 103:1036-1042, 2008
4. Leclercq IA, Da Silva Morais A, Schroyen B, Van Hul N, Geerts A: Insulin resistance in hepatocytes and sinusoidal liver cells: mechanisms and consequences. *J Hepatol* 47:142-156, 2007
5. Wieckowska A, Papouchado BG, Li Z, Lopez R, Zein NN, Feldstein AE: Increased hepatic and circulating interleukin-6 levels in human nonalcoholic steatohepatitis. *Am J Gastroenterol* 103:1372-1379, 2008
6. Ellingsgaard H, Ehses JA, Hammar EB, Van Lommel L, Quintens R, Martens G, Kerr-Conte J, Pattou F, Berney T, Pipeleers D, Halban PA, Schuit FC, Donath MY: Interleukin-6 regulates pancreatic alpha-cell mass expansion. *Proc Natl Acad Sci U S A* 105:13163-13168, 2008
7. Wolf J, Rose-John S, Garbers C: Interleukin-6 and its receptors: a highly regulated and dynamic system. *Cytokine* 70:11-20, 2014
8. Febbraio MA: gp130 receptor ligands as potential therapeutic targets for obesity. *J Clin Invest* 117:841-849, 2007
9. White UA, Stephens JM: The gp130 receptor cytokine family: regulators of adipocyte development and function. *Curr Pharm Des* 17:340-346, 2011
10. Yeoh GC, Ernst M, Rose-John S, Akhurst B, Payne C, Long S, Alexander W, Croker B, Grail D, Matthews VB: Opposing roles of gp130-mediated STAT-3 and ERK-1/ 2 signaling in liver progenitor cell migration and proliferation. *Hepatology* 45:486-494, 2007
11. Franckhauser S, Elias I, Rotter Sopasakis V, Ferre T, Nagaev I, Andersson CX, Agudo J, Ruberte J, Bosch F, Smith U: Overexpression of Il6 leads to hyperinsulinaemia, liver inflammation and reduced body weight in mice. *Diabetologia* 51:1306-1316, 2008
12. Klover PJ, Zimmers TA, Koniaris LG, Mooney RA: Chronic exposure to interleukin-6 causes hepatic insulin resistance in mice. *Diabetes* 52:2784-2789, 2003
13. Wunderlich FT, Strohle P, Konner AC, Gruber S, Tovar S, Bronneke HS, Juntti-Berggren L, Li LS, van Rooijen N, Libert C, Berggren PO, Bruning JC: Interleukin-6 signaling in liver-parenchymal cells suppresses hepatic inflammation and improves systemic insulin action. *Cell Metab* 12:237-249, 2010
14. van Hall G, Steensberg A, Sacchetti M, Fischer C, Keller C, Schjerling P, Hiscock N, Moller K, Saltin B, Febbraio MA, Pedersen BK: Interleukin-6 stimulates lipolysis and fat oxidation in humans. *J Clin Endocrinol Metab* 88:3005-3010, 2003
15. Wueest S, Item F, Boyle CN, Jirkof P, Cesarovic N, Ellingsgaard H, Boni-Schnetzler M, Timper K, Arras M, Donath MY, Lutz TA, Schoenle EJ, Konrad D: Interleukin-6 contributes to early fasting-induced free fatty acid mobilization in mice. *Am J Physiol Regul Integr Comp Physiol* 306:R861-867, 2014

16. Perry RJ, Camporez JP, Kursawe R, Titchenell PM, Zhang D, Perry CJ, Jurczak MJ, Abudukadier A, Han MS, Zhang XM, Ruan HB, Yang X, Caprio S, Kaech SM, Sul HS, Birnbaum MJ, Davis RJ, Cline GW, Petersen KF, Shulman GI: Hepatic Acetyl CoA Links Adipose Tissue Inflammation to Hepatic Insulin Resistance and Type 2 Diabetes. *Cell* 160:745-758, 2015
17. Lam YY, Ha CW, Campbell CR, Mitchell AJ, Dinudom A, Oscarsson J, Cook DI, Hunt NH, Caterson ID, Holmes AJ, Storlien LH: Increased gut permeability and microbiota change associate with mesenteric fat inflammation and metabolic dysfunction in diet-induced obese mice. *PloS One* 7:e34233, 2012
18. Li H, Lelliott C, Hakansson P, Ploj K, Tuneld A, Verolin-Johansson M, Benthem L, Carlsson B, Storlien L, Michaelsson E: Intestinal, adipose, and liver inflammation in diet-induced obese mice. *Metabolism* 57:1704-1710, 2008
19. de Guia RM, Rose AJ, Sommerfeld A, Seibert O, Strzoda D, Zota A, Feuchter Y, Krones-Herzig A, Sijmonsma T, Kirilov M, Sticht C, Gretz N, Dallinga-Thie G, Diederichs S, Kloting N, Bluher M, Berriel Diaz M, Herzig S: microRNA-379 couples glucocorticoid hormones to dysfunctional lipid homeostasis. *EMBO J* 34:344-360, 2015
20. Kloting N, Fasshauer M, Dietrich A, Kovacs P, Schon MR, Kern M, Stumvoll M, Bluher M: Insulin-sensitive obesity. *Am J Physiol Endocrinol Metab* 299:E506-515, 2010
21. Bluher M, Unger R, Rassoul F, Richter V, Paschke R: Relation between glycaemic control, hyperinsulinaemia and plasma concentrations of soluble adhesion molecules in patients with impaired glucose tolerance or Type II diabetes. *Diabetologia* 45:210-216, 2002
22. Betz UA, Bloch W, van den Broek M, Yoshida K, Taga T, Kishimoto T, Addicks K, Rajewsky K, Muller W: Postnatally induced inactivation of gp130 in mice results in neurological, cardiac, hematopoietic, immunological, hepatic, and pulmonary defects. *J Exp Med* 188:1955-1965, 1998
23. Chin SH, Item F, Wueest S, Zhou Z, Wiedemann MS, Gai Z, Schoenle EJ, Kullak-Ublick GA, Al-Hasani H, Konrad D: Opposing effects of reduced kidney mass on liver and skeletal muscle insulin sensitivity in obese mice. *Diabetes* 64:1131-1141, 2015
24. Fisher SJ, Kahn CR: Insulin signaling is required for insulin's direct and indirect action on hepatic glucose production. *J Clin Invest* 111:463-468, 2003
25. Kim JK, Michael MD, Previs SF, Peroni OD, Mauvais-Jarvis F, Neschen S, Kahn BB, Kahn CR, Shulman GI: Redistribution of substrates to adipose tissue promotes obesity in mice with selective insulin resistance in muscle. *J Clin Invest* 105:1791-1797, 2000
26. Wueest S, Yang X, Liu J, Schoenle EJ, Konrad D: Inverse regulation of basal lipolysis in perigonadal and mesenteric fat depots in mice. *Am J Physiol Endocrinol Metab* 302:E153-160, 2012
27. Wiedemann MS, Wueest S, Grob A, Item F, Schoenle EJ, Konrad D: Short-term HFD does not alter lipolytic function of adipocytes. *Adipocyte* 3:115-120, 2014
28. Wueest S, Rapold RA, Schumann DM, Rytka JM, Schildknecht A, Nov O, Chervonsky AV, Rudich A, Schoenle EJ, Donath MY, Konrad D: Deletion of Fas in adipocytes relieves adipose tissue inflammation and hepatic manifestations of obesity in mice. *J Clin Invest* 120:191-202, 2010

29. Konrad D, Rudich A, Schoenle EJ: Improved glucose tolerance in mice receiving intraperitoneal transplantation of normal fat tissue. *Diabetologia* 50:833-839, 2007
30. Wueest S, Rapold RA, Rytka JM, Schoenle EJ, Konrad D: Basal lipolysis, not the degree of insulin resistance, differentiates large from small isolated adipocytes in high-fat fed mice. *Diabetologia* 52:541-546, 2009
31. Pfaffl MW: A new mathematical model for relative quantification in real-time RT-PCR. *Nucleic Acids Res* 29:e45, 2001
32. Knight JA, Anderson S, Rawle JM: Chemical basis of the sulfo-phospho-vanillin reaction for estimating total serum lipids. *Clin Chem* 18:199-202, 1972
33. Bligh EG, Dyer WJ: A rapid method of total lipid extraction and purification. *Can J Biochem Physiol* 37:911-917, 1959
34. Nguyen MT, Favelyukis S, Nguyen AK, Reichart D, Scott PA, Jenn A, Liu-Bryan R, Glass CK, Neels JG, Olefsky JM: A subpopulation of macrophages infiltrates hypertrophic adipose tissue and is activated by free fatty acids via Toll-like receptors 2 and 4 and JNK-dependent pathways. *J Biol Chem* 282:35279-35292, 2007
35. Konrad D, Wueest S: The gut-adipose-liver axis in the metabolic syndrome. *Physiology* 29:304-313, 2014
36. Gao D, Nong S, Huang X, Lu Y, Zhao H, Lin Y, Man Y, Wang S, Yang J, Li J: The effects of palmitate on hepatic insulin resistance are mediated by NADPH Oxidase 3-derived reactive oxygen species through JNK and p38MAPK pathways. *J Biol Chem* 285:29965-29973, 2010
37. Liu HY, Collins QF, Xiong Y, Moukdar F, Lupo EG, Jr., Liu Z, Cao W: Prolonged treatment of primary hepatocytes with oleate induces insulin resistance through p38 mitogen-activated protein kinase. *J Biol Chem* 282:14205-14212, 2007
38. Senn JJ, Klover PJ, Nowak IA, Zimmers TA, Koniaris LG, Furlanetto RW, Mooney RA: Suppressor of cytokine signaling-3 (SOCS-3), a potential mediator of interleukin-6-dependent insulin resistance in hepatocytes. *J Biol Chem* 278:13740-13746, 2003
39. Perry RJ, Samuel VT, Petersen KF, Shulman GI: The role of hepatic lipids in hepatic insulin resistance and type 2 diabetes. *Nature* 510:84-91, 2014
40. Donnelly KL, Smith CI, Schwarzenberg SJ, Jessurun J, Boldt MD, Parks EJ: Sources of fatty acids stored in liver and secreted via lipoproteins in patients with nonalcoholic fatty liver disease. *J Clin Invest* 115:1343-1351, 2005
41. Kawano Y, Cohen DE: Mechanisms of hepatic triglyceride accumulation in non-alcoholic fatty liver disease. *J Gastroenterol* 48:434-441, 2013
42. Summers SA: Ceramides in insulin resistance and lipotoxicity. *Prog Lipid Res* 45:42-72, 2006
43. Fried SK, Bunkin DA, Greenberg AS: Omental and subcutaneous adipose tissues of obese subjects release interleukin-6: depot difference and regulation by glucocorticoid. *J Clin Endocrinol Metab* 83:847-850, 1998
44. Thorne A, Lofgren P, Hoffstedt J: Increased visceral adipocyte lipolysis--a pathogenic role in nonalcoholic fatty liver disease? *J Clin Endocrinol Metab* 95:E209-213, 2010
45. Banke E, Rodstrom K, Ekelund M, Dalla-Riva J, Lagerstedt JO, Nilsson S, Degerman E, Lindkvist-Petersson K, Nilson B: Superantigen activates the gp130 receptor on adipocytes resulting in altered adipocyte metabolism. *Metabolism* 63:831-840, 2014

46. Amar J, Chabo C, Waget A, Klopp P, Vachoux C, Bermudez-Humaran LG, Smirnova N, Berge M, Sulpice T, Lahtinen S, Ouwehand A, Langella P, Rautonen N, Sansonetti PJ, Burcelin R: Intestinal mucosal adherence and translocation of commensal bacteria at the early onset of type 2 diabetes: molecular mechanisms and probiotic treatment. *EMBO Mol Med* 3:559-572, 2011
47. Bervoets L, Van Hoorenbeeck K, Kortleven I, Van Noten C, Hens N, Vael C, Goossens H, Desager KN, Vankerckhoven V: Differences in gut microbiota composition between obese and lean children: a cross-sectional study. *Gut Pathog* 5:10, 2013
48. Kraakman MJ, Kammoun HL, Allen TL, Deswaerte V, Henstridge DC, Estevez E, Matthews VB, Neill B, White DA, Murphy AJ, Peijs L, Yang C, Risis S, Bruce CR, Du XJ, Bobik A, Lee-Young RS, Kingwell BA, Vasanthakumar A, Shi W, Kallies A, Lancaster GI, Rose-John S, Febbraio MA: Blocking IL-6 trans-signaling prevents high-fat diet-induced adipose tissue macrophage recruitment but does not improve insulin resistance. *Cell Metab* 21:403-416, 2015
49. Park SK, Oh SY, Lee MY, Yoon S, Kim KS, Kim JW: CCAAT/enhancer binding protein and nuclear factor-Y regulate adiponectin gene expression in adipose tissue. *Diabetes* 53:2757-2766, 2004
50. Nielsen S, Guo Z, Johnson CM, Hensrud DD, Jensen MD: Splanchnic lipolysis in human obesity. *J Clin Invest* 113:1582-1588, 2004
51. Frayn KN: Visceral fat and insulin resistance--causative or correlative? *Br J Nutr* 83 Suppl 1:S71-77, 2000
52. O'Neill SM, Hinkle C, Chen SJ, Sandhu A, Hovhannisyan R, Stephan S, Lagor WR, Ahima RS, Johnston JC, Reilly MP: Targeting adipose tissue via systemic gene therapy. *Gene Ther* 21:653-661, 2014
53. Uhrig-Schmidt S, Geiger M, Luippold G, Birk G, Mennerich D, Neubauer H, Grimm D, Wolfrum C, Kreuz S: Gene delivery to adipose tissue using transcriptionally targeted rAAV8 vectors. *PLoS One* 9:e116288, 2014

Figure Legends

Figure 1 Similar weight gain and adipogenesis in gp130$^{F/F}$ and gp130$^{\Delta adipo}$ mice

(**A**) Western blot analysis of gp130 protein levels in respective cells and tissues of gp130$^{F/F}$ and gp130$^{\Delta adipo}$ mice. (**B**) Body weight of chow (circles) and HFD-fed (squares) gp130$^{F/F}$ and gp130$^{\Delta adipo}$ mice. n=5-24. Fat pad weights of epididymal (**C**) and mesenteric (**D**) depots of chow and HFD-fed gp130$^{F/F}$ and gp130$^{\Delta adipo}$ mice**.** n=6-18. Diameter of epididymal (**E**) and mesenteric (**F**) adipocytes of chow (circles) and HFD-fed (squares) gp130$^{F/F}$ and gp130$^{\Delta adipo}$ mice. n=4-6. Results are the means ± SEM. F/F: gp130$^{F/F}$; ∆ad: gp130$^{\Delta adipo}$. ***p < 0.001, **p < 0.01, *p < 0.05 (ANOVA).

Figure 2 Reduced basal lipolysis and portal FFA levels in obese gp130$^{\Delta adipo}$ mice

Basal FFA release from epididymal (**A**) and mesenteric (**B**) adipocytes of chow and HFD-fed gp130$^{F/F}$ and gp130$^{\Delta adipo}$ mice. n=5-10. Protein levels of phospho-ERK, ERK and actin in epididymal (**C**) and mesenteric (**D**) WAT of HFD-fed gp130$^{F/F}$ and gp130$^{\Delta adipo}$ mice. n=4. FFA concentration was determined in systemic (**E**) and portal (**F**) plasma samples of chow and HFD-fed gp130$^{F/F}$ and gp130$^{\Delta adipo}$ mice. n=3-8. IL-6 (**G**) as well as CD11b and F4/80 (**H**) mRNA expression in mesenteric fat of HFD-fed gp130$^{F/F}$ and gp130$^{\Delta adipo}$ mice. n=6. Results are the means ± SEM. F/F: gp130$^{F/F}$; ∆ad: gp130$^{\Delta adipo}$. ***p < 0.001, **p < 0.01, *p < 0.05 (Student's *t* test for Fig. D or ANOVA for Figs. A, B, E and F).

Figure 3 Reduced hepatic steatosis in HFD-fed gp130$^{\Delta adipo}$ mice

(**A**) Protein levels of phospho-p38 and actin in livers of HFD-fed gp130$^{F/F}$ and gp130$^{\Delta adipo}$ mice. n=10. (**B**) Protein levels of SOCS and actin in livers of HFD-fed gp130$^{F/F}$ and gp130$^{\Delta adipo}$ mice. n=6. (**C** and **D**) Total liver lipid and liver triglyceride (TG) levels of chow and HFD-fed gp130$^{F/F}$ and gp130$^{\Delta adipo}$ mice. n=4-6. (**E**) Representative histological hematoxylin- and eosin-stained liver sections of HFD-fed gp130$^{F/F}$ and gp130$^{\Delta adipo}$ mice. (**F and G**) mRNA expression of respective genes in livers HFD-fed gp130$^{F/F}$ and gp130$^{\Delta adipo}$ mice. n=10. Results are the means ± SEM. F/F: gp130$^{F/F}$; Δad: gp130$^{\Delta adipo}$. *p < 0.05 (Student's *t* test).

Figure 4 Improved hepatic insulin sensitivity in HFD-fed gp130$^{\Delta adipo}$ mice

Glucose infusion rate (GIR) (**A**), endogenous glucose production (EGP) (**B**) and glucose uptake into quadriceps muscle (**C**) during hyperinsulinemic-euglycemic clamps in HFD-fed gp130$^{F/F}$ and gp130$^{\Delta adipo}$ mice. n=4-6. Insulin-inhibited FFA release from epididymal (**D**) and mesenteric (**E**) adipocytes of HFD-fed gp130$^{F/F}$ and gp130$^{\Delta adipo}$ mice. n=8-10. Results are the means ± SEM. F/F: gp130$^{F/F}$; Δad: gp130$^{\Delta adipo}$. **p < 0.01, *p < 0.05 (Student's *t* test).

Figure 5 Positive correlation of omental IL-6 expression with hepatic steatosis and insulin resistance in humans

(**A**) *IL-6* mRNA expression in omental and subcutaneous (sc) white adipose tissue (WAT) of lean (n=12) and obese (n=51) human subjects. Omental *IL-6* mRNA expression correlates with liver fat content (**B**) and glucose infusion rate (GIR) during the

steady state of a euglycemic-hyperinsulinemic clamp (**C**). Results are the means ± SEM.

$^{\#}p=0.11$ (Student's *t* test).

Table 1 Basal clinical characteristics of human subjects

	Lean (n=12)	Overweight/Obese (n=51)
Age (years)	62±12	70±12
Men/Women (n)	8/4	26/25
Type 2 diabetes (n)	0	22
Body mass index (kg/m²)	24.5±0.2	34.4±0.8***
Body fat (%)	22.4±0.5	36.7±1.3***
Liver fat content (%)	2.0±0.1	22.5±1.8***
Fasting plasma glucose (mmol/l)	5.3±0.1	5.7±0.1
Fasting plasma insulin (pmol/l)	16.8±3.5	204.1±19.1***
Glucose infusion rate, clamp (µmol/kg/min)	101.2±3.3	49.7±3.5***
HbA1c (%)	5.28±0.05	5.81±0.07***
Total cholesterol (mmol/l)	4.42±0.19	5.42±0.12***
LDL-cholesterol (mmol/l)	2.74±0.26	3.13±0.13
HDL-cholesterol (mmol/l)	1.45±0.1	1.32±0.03
Triglycerides (mmol/l)	0.9±0.12	2.08±0.1***
Free fatty acids (mmol/l)	0.38±0.06	0.63±0.04*
IL-6 (pmol/l)	1.11±0.24	3.87±0.39**
Adiponectin (ng/ml)	9.27±1.25	4.49±0.35**
Leptin (ng/ml)	4.75±1.15	26.9±1.91***

*p<0.05, **p<0.01, ***p<0.001 for comparisons between lean and obese individuals.

Data are given as mean ± SEM.

Figure 1

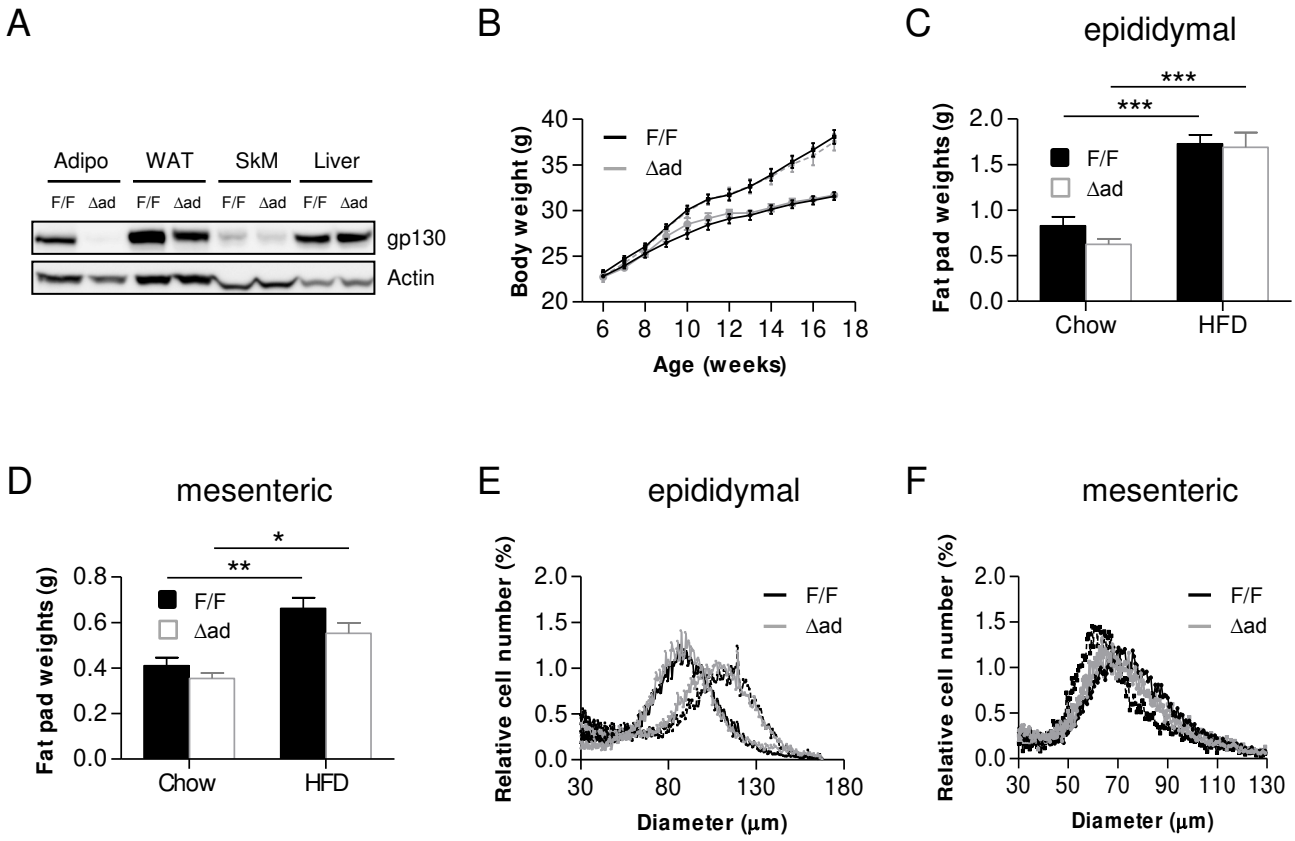
A
Adipo
WAT
SkM
Liver
F/F
Δad
gp130
Actin
B
Body weight (g)
Age (weeks)
F/F
Δad
C
epididymal
Fat pad weights (g)
Chow
HFD
***
D
mesenteric
*
**
E
epididymal
Relative cell number (%)
Diameter (μm)
F
mesenteric

Figure 2

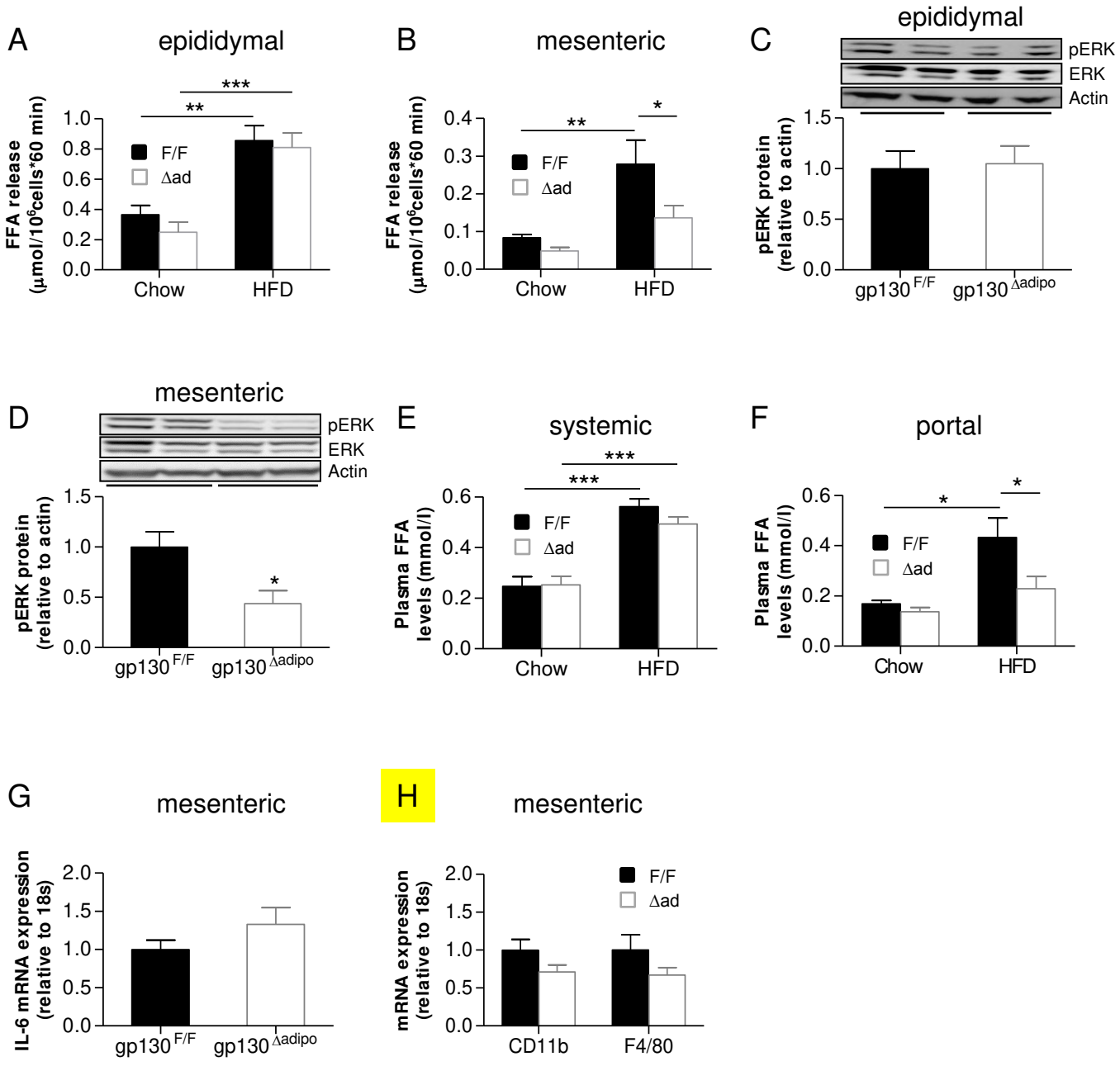
A
epididymal
FFA release (µmol/10^6cells*60 min)
F/F
Δad
Chow
HFD
B
mesenteric
C
epididymal
pERK
ERK
Actin
pERK protein (relative to actin)
gp130 F/F
gp130 Δadipo
D
mesenteric
E
systemic
Plasma FFA levels (mmol/l)
F
portal
G
mesenteric
IL-6 mRNA expression (relative to 18s)
H
mesenteric
mRNA expression (relative to 18s)
CD11b
F4/80

Figure 3

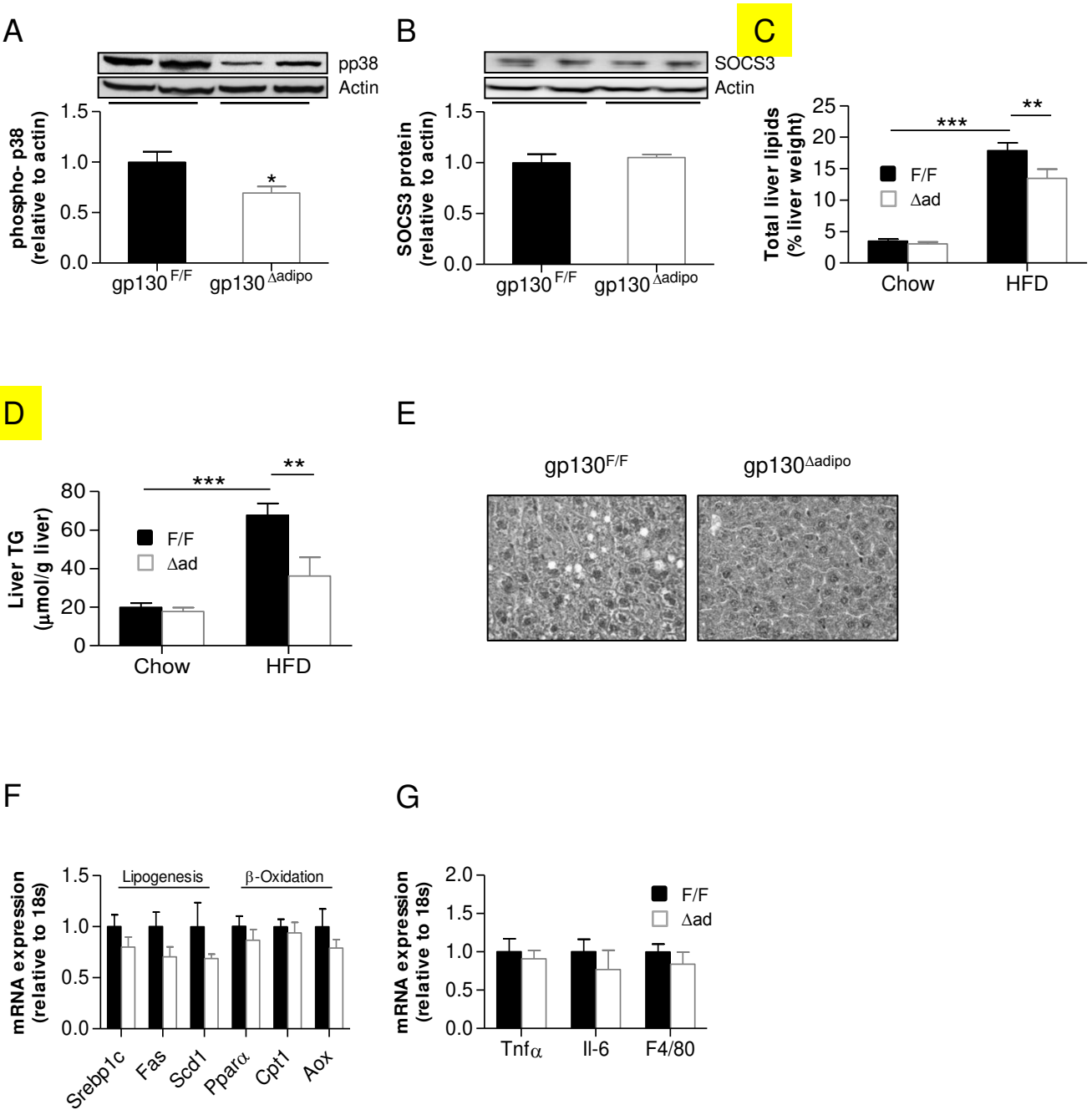
A
pp38
Actin
phospho- p38 (relative to actin)
1.5
1.0
0.5
0.0
*
gp130 F/F
gp130 Δadipo
B
SOCS3
Actin
SOCS3 protein (relative to actin)
1.5
1.0
0.5
0.0
gp130 F/F
gp130 Δadipo
C
Total liver lipids (% liver weight)
25
20
15
10
5
0
***
**
F/F
Δad
Chow
HFD
D
Liver TG (µmol/g liver)
80
60
40
20
0
***
**
F/F
Δad
Chow
HFD
E
gp130F/F
gp130Δadipo
F
mRNA expression (relative to 18s)
1.5
1.0
0.5
0.0
Lipogenesis
β-Oxidation
Srebp1c
Fas
Scd1
Pparα
Cpt1
Aox
G
mRNA expression (relative to 18s)
2.0
1.5
1.0
0.5
0.0
F/F
Δad
Tnfα
Il-6
F4/80

Figure 4

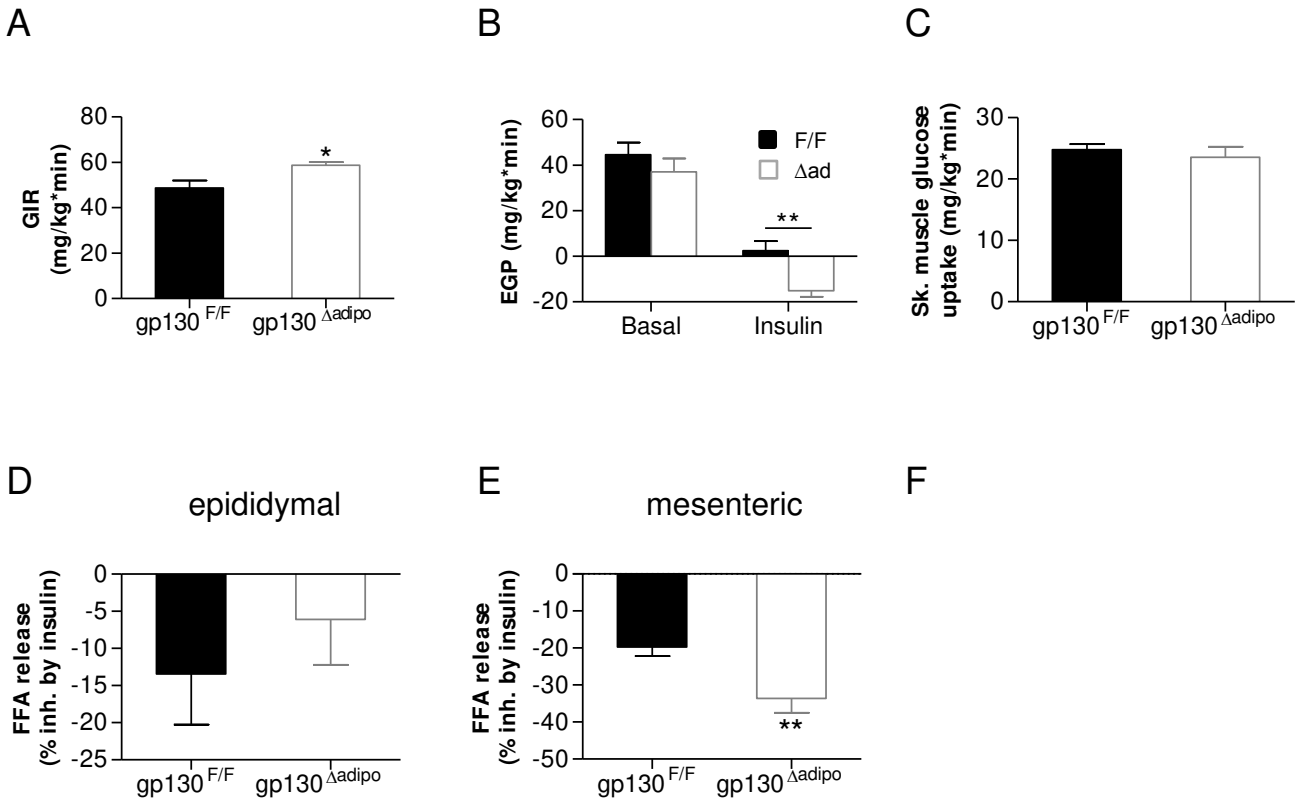
A
GIR (mg/kg*min)
80
60
40
20
0
*
gp130 F/F
gp130 Δadipo
B
EGP (mg/kg*min)
60
40
20
0
-20
F/F
Δad
**
Basal
Insulin
C
Sk. muscle glucose uptake (mg/kg*min)
30
20
10
0
gp130 F/F
gp130 Δadipo
D
epididymal
FFA release (% inh. by insulin)
0
-5
-10
-15
-20
-25
gp130 F/F
gp130 Δadipo
E
mesenteric
FFA release (% inh. by insulin)
0
-10
-20
-30
-40
-50
**
gp130 F/F
gp130 Δadipo
F

Figure 5

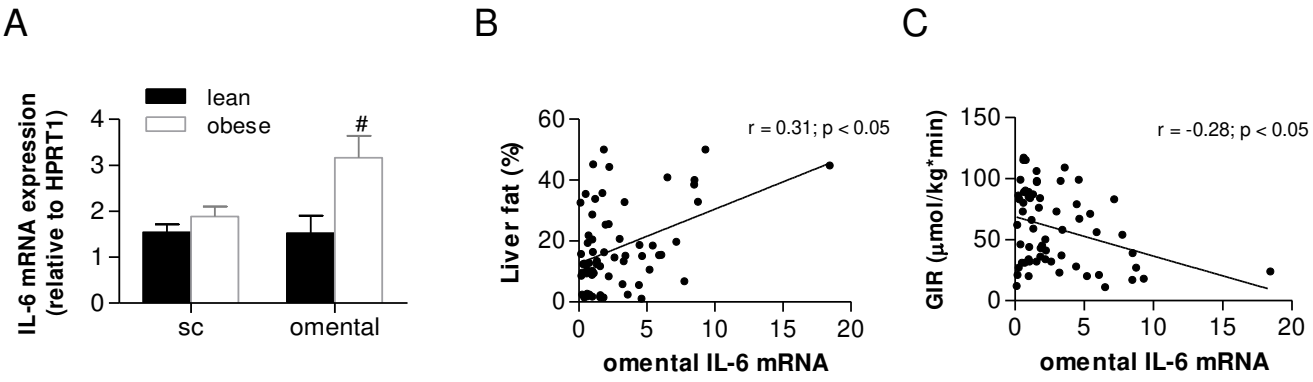
A
B
C
IL-6 mRNA expression (relative to HPRT1)
lean
obese
#
sc
omental
Liver fat (%)
r = 0.31; p < 0.05
omental IL-6 mRNA
GIR (µmol/kg*min)
r = -0.28; p < 0.05
omental IL-6 mRNA

Supplemental Figure 1

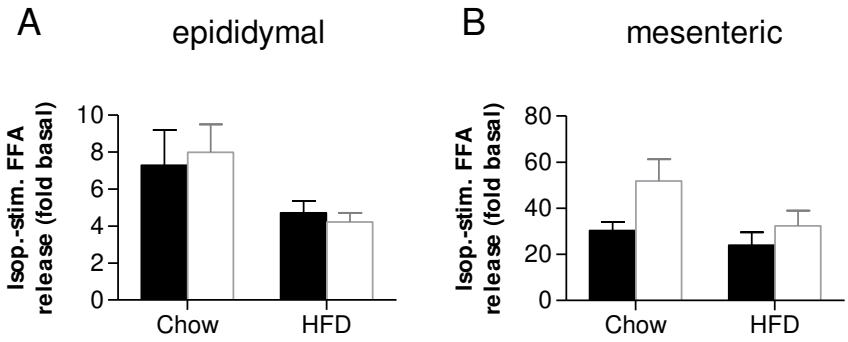

Isoproterenol-stimulated lipolysis in adipose tissue of gp130$^{F/F}$ and gp130$^{\Delta adipo}$ mice

Isoproterenol-stimulated FFA release (fold over basal) from epididymal (**A**) and mesenteric (**B**) adipocytes of chow and HFD-fed gp130$^{F/F}$ (black bars) and gp130$^{\Delta adipo}$ (open bars) mice. n=5-10. Results are the means ± SEM.

Supplemental Figure 2

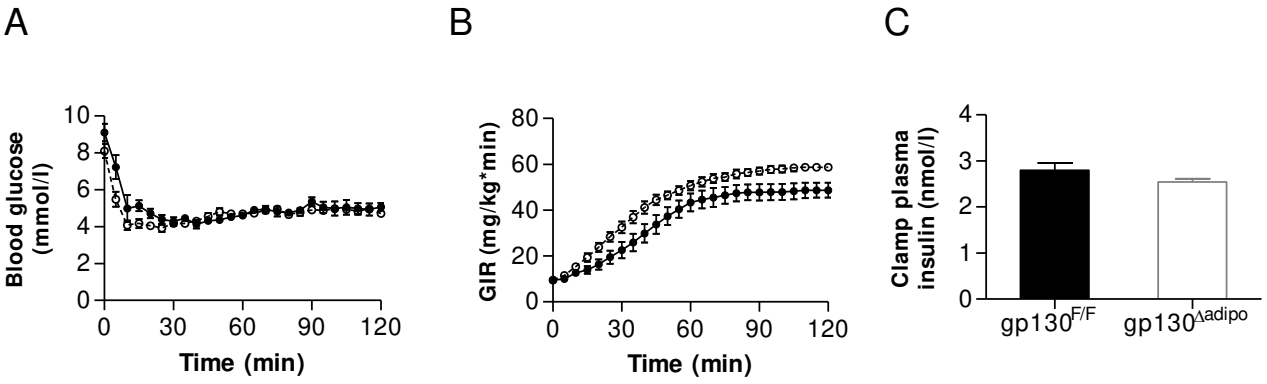

Blood glucose concentrations, glucose infusion rates and plasma insulin levels during hyperinsulinemic-euglycemic clamp

(**A**) Blood glucose levels were clamped upon insulin infusion at about 5 mmol/l in HFD-fed gp130$^{F/F}$ (black circles) and gp130$^{\Delta adipo}$ (open circles) mice. n=6. (**B**) In order to maintain euglycemia, glucose infusion rate was adjusted over time in gp130$^{F/F}$ (black circles) and gp130$^{\Delta adipo}$ (black circles) mice. n=6. (**C**) Plasma insulin levels after insulin infusion. n=4-5. Results are the means ± SEM.

Supplemental Figure 3

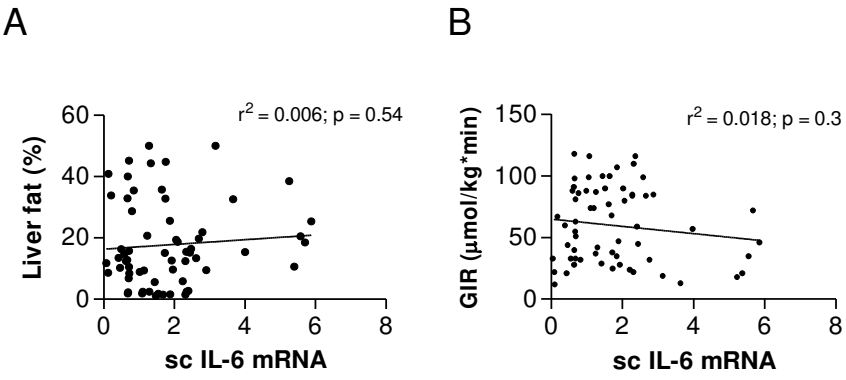

Absent correlation between subcutaneous IL-6 expression and liver fat content

Subcutaneous IL-6 mRNA expression was determined in lean and obese human subjects and correlated to liver fat content (**A**) and glucose infusion rate (GIR) (**B**). n= 63.